Renewable and Sustainable Energy Reviews 61 (2016) 213–221

Contents lists available at ScienceDirect

Renewable and Sustainable Energy Reviews

journal homepage: www.elsevier.com/locate/rser

Methods and techniques to determine the dynamic parameters of solar cells: Review

D.T. Cotfas [a,*], P.A. Cotfas [a], S. Kaplanis [b]

[a] Transilvania University of Brasov/DEC Department, Brasov, Romania
[b] Technological and Educational Institute of Western Greece, Greece

ARTICLE INFO

Article history:
Received 7 April 2015
Received in revised form
30 January 2016
Accepted 25 March 2016
Available online 12 April 2016

Keywords:
Solar cells
Ac and dc parameters
Impedance spectroscopy
Time domain
C–V characteristic

ABSTRACT

The new types of solar cells, such as thin film, dye sensitized, organic and multi-junction are increasingly being used. The behavior of these solar cells in dynamic regime differs from the one of the mono-crystalline or polycrystalline solar cells. The review article critically outlines and discusses the main issues of the ten methods which have been presented in the research literature in previous years in order to analyze the dynamic behavior of solar cells. This paper presents the methods which allow the determination of either of all ac parameters of solar cells or only one of them. The methods analyzed allow measuring the dynamic impedances using the frequency and time domain techniques. It also discusses the methodologies to determine the dc parameters of solar cells from the variation of the capacitance applying reverse and forward bias. The different types of the solar cells ac equivalent circuits from a proper fitting are also discussed in this review. The paper presents pros and cons for each one of the ten methods allowing the determination of the ac parameters and some dc parameters of solar cells.

Contents

1. Introduction

The renewable energy is nowadays universally recognized as the main resource towards sustainability. The world is now more than ever energy conscious, due to the climatic changes. The need to live in an unpolluted world is a sine qua non and therefore extensive investments are made in renewable energy [1].

The determination of the electric parameters in any PV cell and module under any field conditions has been extensively studied especially under steady state conditions [2], but also transient conditions even at various solar radiation levels [3–10].

The dc parameters of any PV module attracted the interest as the PV panels produce dc current. However, the majority of the applications require current in ac form. The design of PV

* Corresponding author.
E-mail address: dtcotfas@unitbv.ro (D.T. Cotfas).

http://dx.doi.org/10.1016/j.rser.2016.03.051
1364-0321/

generators show diversified configurations. These include the power conditioning unit with charge controllers DC/AC inverters, switches, MPPT devices, battery storage systems in stand-alone PV systems, etc. For understanding the behavior of the photovoltaic cells and modules in various configurations it is useful to analyze and study their ac parameters.

Using proper mathematical models and the *I–V* characteristic, the important dc parameters of solar cells can be determined by more than 35 methods outlined in [2]. These parameters are: I_{ph} – the photogenerated current, I_{sc} – the short circuit current, V_{oc} – the open circuit voltage, n – the ideality factor of diode, R_s – the series resistance, R_{sh} – the shunt resistance, I_o – the reverse saturation current and P_m – the maximum power [2].

On the other hand, the dynamic regime of the solar cells was less studied until some years ago in comparison to the static regime [5]. Nowadays, due to the development of new types of photovoltaic cells and of a large number of photovoltaic power plants, the research reports published methods on studies of the ac behavior and the determination of the ac parameters of solar cells and modules [3–14].

The paper is structured as follows: in Section 2 the ac parameters of solar cells and the equivalent circuit in dynamic regime are outlined; Section 3 shortly presents the experimental methodologies along with the associated mathematical expressions which allow for the determination of the ac parameters of the solar cell. In Section 4 those methodologies are discussed. A comparison is given with arguments about the pros and cons for each method; the complex equivalent circuits for the determination of the ac parameters through fitting are presented, the application of suitable methodologies to new types of solar cells is argued, and the necessity to understand the dynamic behavior of the solar cells is explained. Finally, the Conclusions are presented in Section 5.

2. Electric equivalent circuits for the dynamic simulation of a PV cell

The solar cell electric equivalent circuit in dynamic regime is obtained from the dc one diode equivalent circuit by replacing the diode with the diffusion capacitance C_d, the transition capacitance C_t and the dynamic resistance of diode R_d, see Fig. 1a. The dynamic equivalent circuit can be simplified using the parallel resistance R_p which is the result of combining R_d with R_{sh} and the parallel capacitance C_p which is the result of combining C_d with C_t, see Fig. 1b. The simplified circuit is frequently used because of its small number of the fitting parameters [6,7].

The transition capacitance of the photovoltaic cell, which is voltage dependent, can be calculated using the following equation for an abrupt junction [5,8]:

$$C_t = \frac{b}{\sqrt{V_j - V_a}} = A\sqrt{\frac{eN\varepsilon_o\varepsilon_r}{2(V_j - V_a)}}, \quad N = \frac{N_D N_A}{N_D + N_A} \tag{1}$$

where b is a constant which depends on the photovoltaic cell, V_j is the junction voltage V_a is the applied voltage, A represents the area

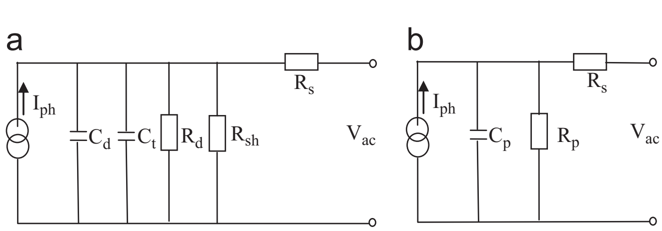

Fig. 1. The ac equivalent circuit and the simplified ac equivalent circuit for a solar cell.

of the solar cell, e is the elementary charge, ε_o is the permittivity of free space, ε_r represents the relative permittivity of the solar cell material, N_D and N_A are the doping concentration in cm^{-3} in the n and p region, respectively.

The diffusion capacitance of the photovoltaic cell, which is frequency and voltage dependent [8], can be determined by the following equation:

$$C_d = \frac{\tau e}{2kT} I_o \exp\left(\frac{eV_a}{nkT}\right), \quad w\tau << 1 \tag{2}$$

where τ represents the minority carrier lifetime, k denotes the Boltzmann constant, T represents the photovoltaic cell temperature, n is the ideality factor of the PV cell diode and w represents the angular frequency.

For the calculation of the dynamic resistance of the photovoltaic cell, which is voltage dependent, the following expression can be used [5]:

$$R_d = \frac{kTn}{eI} \tag{3}$$

The dynamic impedance of the photovoltaic cells or panels in dark conditions under the bias voltage and the signal frequency ω can be calculated using the following equation [4,9]:

$$Z(V,\omega) = R(V,\omega) + jX(V,\omega) = R_s + \left\{ \frac{[R_{sh} + R_d(V)]R_{sh}R_d(V)}{\omega^2 R_{sh}^2 R_d^2(V)[C_d(V,\omega) + C_t(V)]^2 + [R_{sh} + R_d(V)]^2} \right\} - j\left\{ \frac{\omega R_{sh}^2 R_d^2(V)[C_d(V,\omega) + C_t(V)]}{\omega^2 R_{sh}^2 R_d^2(V)[C_d(V,\omega) + C_t(V)]^2 + [R_{sh} + R_d(V)]^2} \right\} \tag{4}$$

Eq. (4) can be rewritten, in case of the simplified ac equivalent circuit, using the formula for parallel connection of resistors and the capacitors [9]:

$$Z(V,\omega) = \left[R_s + \frac{R_p}{(\omega R_p C_p)^2 + 1} \right] - j\left[\frac{\omega {R_p}^2 C_p}{(\omega R_p C_p)^2 + 1} \right] \tag{5}$$

3. Methods used to determine the PV cell ac parameters

Several methods for the determination of the ac parameters of the PV cells have been proposed and studied. Most of them apply the technique of the impedance spectroscopy [6]. The impedance spectroscopy is a powerful technique developed by researchers in the electrochemistry domain [10].

3.1. Methods to determine all ac parameters of solar cells

Method 1 – In this method the impedance spectroscopy with the frequency domain technique is used. The ac signal which is superposed on the dc bias is a pure sinusoidal signal. Its amplitude must be smaller than the thermal voltage, (nkT/e), with a varying frequency. The value of the thermal voltage at the 25 °C is approximately equal to 25.7 mV. The dynamic impedance is measured at different values of the bias voltage, in general from 0 V to the open circuit voltage of the solar cell for forward voltage; the frequency can vary from 1 Hz to 1 MHz. The measurements can be made in dark conditions as well as under different levels of illumination. The results are plotted in a complex impedance plane-impedance loci, Nyquist diagram [11,12], see Fig. 2. The semicircular shape of the plot certifies an ac equivalent circuit with capacitance in parallel to a resistance.

This method, by directly analyzing the plot, allows the determination of the series and the parallel resistance of the photovoltaic cells or panels. For the analysis, the applied bias voltage might be applied in reverse or forward mode.

Fig. 2. The impedance loci of a monocrystalline silicon photovoltaic cell under reverse bias voltage conditions.

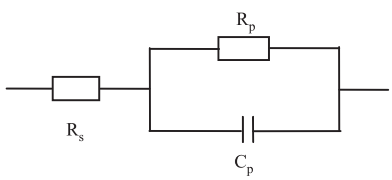

Fig. 3. The equivalent circuit for fitting.

In the case of the reverse mode, Fig. 2, the semicircle intersects the real axis in two points. The series resistance is given by the real coordinate of the point close to the origin point, where the frequency is high. The diameter of the semicircle gives the value of the parallel resistance. Using this reverse mode the shunt resistance can be determined at low levels of bias voltage. The shunt resistance can be considered approximately equal with the parallel resistance, R_p, because the dynamic resistance, R_d, is much greater than the shunt resistance. In the case of the capacitance, the transition capacitance is the dominant term [9].

In the case of the forward mode the series resistance is given as in the previous case. The parallel resistance is given by the value of the semicircle diameter. The parallel resistance can be considered as the dynamic resistance, because the shunt resistance has a big value and it can be neglected [11]. As it concerns the capacitance, the diffusion capacitance is the predominant one [9].

The experimental data obtained are fitted using the equivalent circuit of the solar cells, Fig. 3. The different devices used to measure the dynamic impedance come with software application that implement the fitting procedure. In this application, the complex nonlinear regression least-squares algorithm is generally used.

The following parameters can be obtained by the fitting procedure: the series resistance, the parallel resistance and the parallel capacitance. For the case of the bias voltage mode, the parallel resistance can be considered to be the shunt or the dynamic resistance and the parallel capacitance can be considered to be the transition or diffusion capacitance.

Method 2 – Chenvidhya et al. [4] developed a new method to determine the ac parameters of solar cells. The measurements are made in dark conditions using square wave signal, which varied from 1 Hz to 30 kHz, instead of the ac sinusoidal signal. The dynamic impedance of the solar cell can be determined using the FFT technique and the output response. This method allows plotting the Nyquist diagram, as well. The measurement period required is smaller than the one for the impedance spectroscopy with ac sinusoidal signal because the impedance locus is obtained using few square wave inputs, [4]. Chenvidhya et al. state that 2–3 square wave inputs at different frequencies are sufficient to obtain the whole Nyquist diagram. This is based on the spectral composition of the square wave. The response signals, voltage and current, for each applied square wave can be determined by using the Fourier analysis, the amplitudes and phases of several harmonics, up to ten [4]. In this method, the classic devices [4], Fig. 4, or the Frequency response analyser FRA can be used to make the measurements.

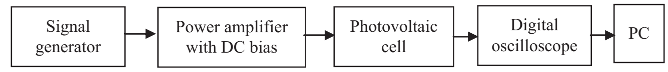

Fig. 4. The experimental set-up [4].

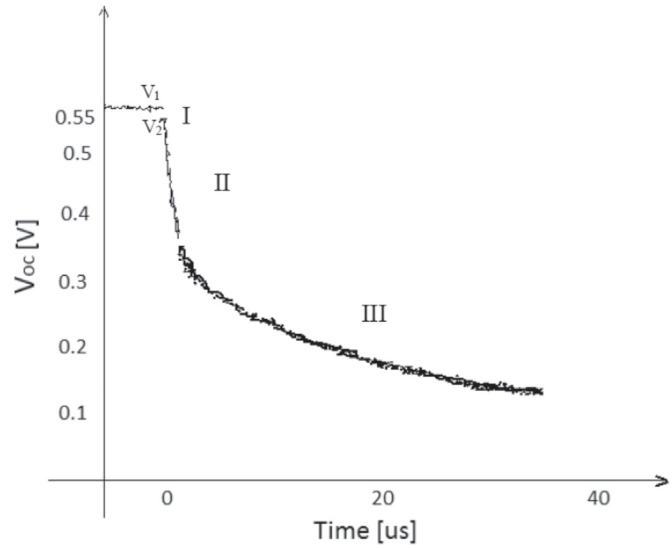

Fig. 5. Open circuit voltage decay [14].

The measurement can be done at different forward biasing in order to study the behavior of the dynamic resistance. The series, shunt and dynamic resistance are obtained in the same manner, as in Method 1, from the Nyquist diagram. The DC resistance, which represents the combined effect of the parasite resistances series and shunt, and the dynamic resistance, can be calculated from the dc terms in the FFT analysis, at any biasing level.

Method 3 – Kumar et al. developed a method to determine the ac parameters of solar cells using the time domain technique [13,14]. The measurements are made in dark conditions. The method consists of applying a constant current in the solar cell, equal with the short circuit current which charges the junction capacitance around the open circuit voltage.

The junction capacitance discharges on the parallel resistance of the solar cell when the current is abruptly terminated and the decay of the voltage can be measured [14]. This voltage decay curve, Fig. 5, has three important regions. The first region is the one where the voltage has a sharp decrease, the second region is the linear part of the curve where the diffusion effect is important and the third region of the curve is the rest of it. The last part of the voltage decay characteristic is not linear due to the depletion effect in the space charge region [15].

The open circuit voltage decay technique – OCVD can be used to calculate the ac parameters and the series resistance of the photovoltaic cells. The series resistance of the photovoltaic cell can be determined using the first region of the voltage decay characteristic and Eq. (6) [14,16]:

$$R_s = \frac{V_1 - V_2}{I_{sc}} \tag{6}$$

where the voltage difference is given by the voltage drop on the series resistance.

The ac parameters R_p and C_p will be calculated for different values of the voltage, using the *I–V* characteristic measured in dark conditions and the other regions of the voltage decay characteristic.

The parallel resistance, R_p, is determined by using Eq. (7)

$$R_p = \frac{R_d R_{sh}}{R_d + R_{sh}} \tag{7}$$

where the dynamic resistance R_d is determined by using Eq. (8) and the shunt resistance is determined by using Eq. (9)

$$R_d = -\frac{1}{dI/dV} \tag{8}$$

where the slope (dI/dV) of the *I–V* characteristic for each voltage is determined with the Savitzky–Golay algorithm [14].

$$R_{sh} = \frac{V}{I} \tag{9}$$

(V,I) is a point of the *I–V* characteristic which corresponds to the applied voltage [14,17].

The diffusion capacitance is dominant for the second region and it is considered to be the parallel capacitance. The diffusion capacitance is calculated using Eq. (10):

$$C_d = \frac{\tau_\upsilon}{R_p} \tag{10}$$

where R_p is the parallel resistance calculated for the voltage V and the effective lifetime τ_υ is calculated using Eq. (11):

$$\tau_\upsilon = \frac{nV_T}{dV_{oc}/dt} \tag{11}$$

where n is the ideality factor of diode, which may be considered equal to 1 or for accurate determination of the effective lifetime it can be determined from the *I–V* characteristic using different methods [5], V_T represents the thermal voltage which can be calculated with Eq. (12), dV_{oc}/dt is the slope of the linear part of the voltage decay characteristic and can be determined using the linear fit of data [14].

$$V_T = \frac{kT}{e} \tag{12}$$

The transition capacitance is dominant in the third region and it is considered as parallel capacitance. The transition capacitance is calculated using Eq. (13):

$$C_t = \frac{1}{(dV/dt)_{V=V_b}} \tag{13}$$

where $(dV/dt)_{V=Vb}$ is the slope of the voltage decay characteristic at voltage bias.

Method 4 – Chenvidhya et al. developed the method which allows the determination of the ac parameters of the solar cell using the time domain responses. The measurements are done in dark conditions using square wave inputs. The time constant of the solar cell equivalent circuit can be determined by Eq. (14) in time domain at any bias voltage or by using the slope determined in the square wave transition point for the time response curve [12].

$$Time\ Constant = \frac{R_s R_{sh} R_d(V)[C_t(V) + C_d(V,\omega)]}{R_d(V)R_{sh} + R_s[R_d(V) + R_{sh}]} \tag{14}$$

From Eq. (14) it is observed that the *Time Constant* depends on the voltage and frequency. The diffusion capacitance is the only term which is frequency dependent.

This method allows the analysis of the dependence of the *Time constant* on the frequency because it uses the square wave signal. The analysis of the dependency between the *Time constant* and frequency under reverse and forward bias proves: the *Time constant* is higher in reverse bias than in forward bias for a photovoltaic cell with low junction quality; it decreases more quickly in lower frequency for reverse bias than for forward bias; it decreases with the voltage increase at the same frequency [16]. It can be concluded that the *Time constant* varies with the voltage and frequency.

3.2. Methods to determine the capacitance of solar cells

Method 5 – Twarowski and Albrecht used the low frequency oscillographic methods to determine directly the organic solar cell capacitance [18]. In this method, an ac sinusoidal or triangular wave signal can be applied. The amplitude and the frequency of the signal can be chosen. The capacitance of the solar cell can be calculated by Eq. (15) for the sinusoidal wave signal and by Eq. (16) for the triangular wave signal:

$$C = \frac{I_+ - I_-}{4\pi f_{in}\sqrt{V_{in}^2 - V^2}} \tag{15}$$

$$C = \frac{I_+ - I_-}{8V_{in}f_{in}} = \frac{\Delta I}{8V_{in}f_{in}} \tag{16}$$

where V_{in} is the amplitude of the sinusoidal or triangular voltage, f_{in} represents the frequency of the applied signal, whereas I_+ and I_- represent the currents measured for a single value of the applied voltage, V.

The experimental setup for the low frequency oscillographic method [18] to measure the current voltage curve of the photovoltaic cells is presented in Fig. 6. The function generator provides the input for the x channel of the oscilloscope and the sinusoidal or triangular voltage for biasing the photovoltaic cell at the desired frequency. The input of the channel y is the amplified voltage drop across R. The resistance R should be chosen so that the voltage drop across the photovoltaic cell must be much higher than the voltage drop across R [18].

Method 6 – Mandal et al. determine the capacitance using low level triangular wave signal of desired amplitude for the GaAs/Ge photovoltaic cells [19] and low sinusoidal wave signal of desired amplitude for the GaAs/Ge and Si (BSFR-back surface field and reflector) photovoltaic cells [20]. The measurements are made in dark conditions and at different temperatures. Using the experimental set-up, see Fig. 7, which allows generating both triangular and sinusoidal wave signals and the equations Eqs. (15) and (16), the capacitance of the solar cell can be calculated by measuring currents I_+ and I_-.

The role of the waveform generator is to produce the triangular or sinusoidal signal with the desired amplitude and frequency. Using the D/A convertor, connected to the waveform generator through a series resistor, the frequency can be adjusted digitally. The solar cell is biased using the DC bias and the power amplifier. The operational amplifier, the absolute value output circuit, peak detector, A/D convertor and microcontroller are used to measure the current at an applied voltage and to measure the capacitance of the solar cell. The role of the thermostat is to keep the solar cell temperature constant during the measurements.

Method 7 – Jeevandoss et al. developed a method to determine the parallel capacitance of the monocrystalline and polycrystalline silicon solar cells though compensation of the parallel resistance effect [21]. The experimental setup for this method is presented in Fig. 8a, allowing the measurement of the *C–V* characteristic. The

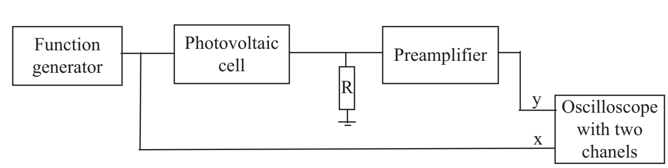

Fig. 6. The experimental setup for measuring the photovoltaic cell capacitance by low frequency oscillographic methods [18].

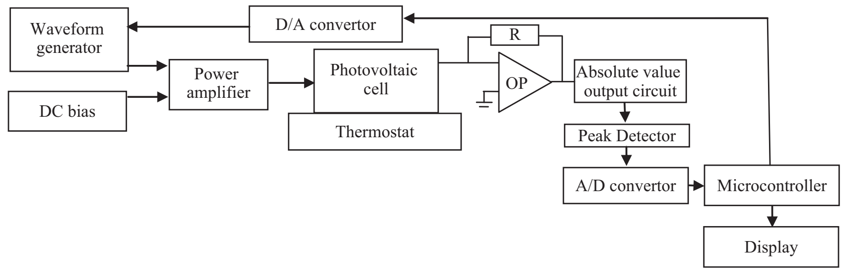

Fig. 7. The experimental setup for measuring the photovoltaic cell capacitance [20].

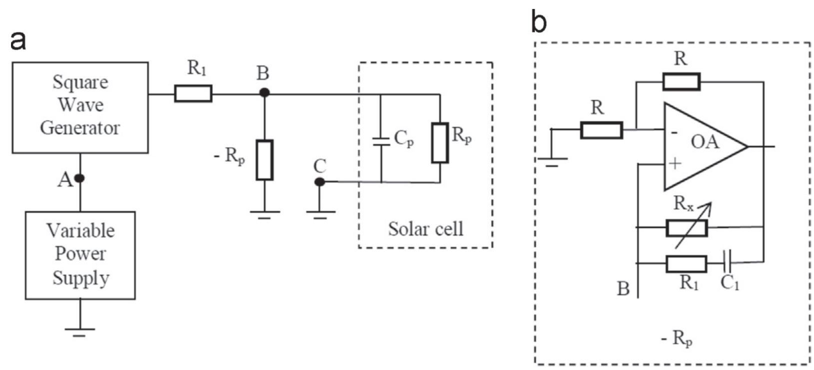

Fig. 8. The experimental setup for measuring the capacitance though compensation of the parallel resistance effect [21].

negative resistance for compensating the parallel resistance of the solar cell is obtained using an Opamp with resistors R, the variable resistance R_x connected in parallel with the series combination between resistance which is equal with R_s and capacitor C_1, see Fig. 8b. It is considered that R_p is nulled when the voltage difference between the nodes A and B equals zero and this can be obtained through variation of the R_x. If the R_p is nulled then only C_p influences the measurements between terminals B and C. The variable power supply is a dc source used together with a generator which provides a symmetrical square wave current to excite the solar cell and the negative parallel resistance, Fig. 8a.

The parallel capacitance can be calculated using the following equation:

$$C_p = \frac{T_s I_s}{4V_p} \tag{17}$$

where I_s is the magnitude of the symmetrical square wave current, T_s is the period of the square wave and the V_p is the peak voltage of the parallel capacitor.

The experimental setup allows for measuring the C–V characteristic in both reverse and forward bias conditions, by changing the polarity of the variable power supply. The capacitance frequency characteristic can be obtained if the T_s is varied and the bias voltage is maintained constant.

Because the series resistance is not taken into account in the equivalent circuit of the solar cell, this can introduce errors in measurements. The measurement errors for parallel capacitance in reverse bias are negligible, because the series resistance is very small in comparison with the parallel resistance. The parallel resistance in forward bias is in the order of ohms and introduce errors for R_p measurements. For the parallel capacitance the errors are negligible because both parallel and series resistances are compensated by variation of R_x.

Method 8 – The C–V characteristic for the solar cells can be measured in both reverse and forward bias conditions [8]. The semi logarithmic C–V characteristic is split in two regions, as shown in Fig. 9. In the second region the diffusion capacitance is dominant. The applied voltage for this region is over 0.2 V [8]. Applying the logarithm in both sides of Eq. (2), the following expression is obtained:

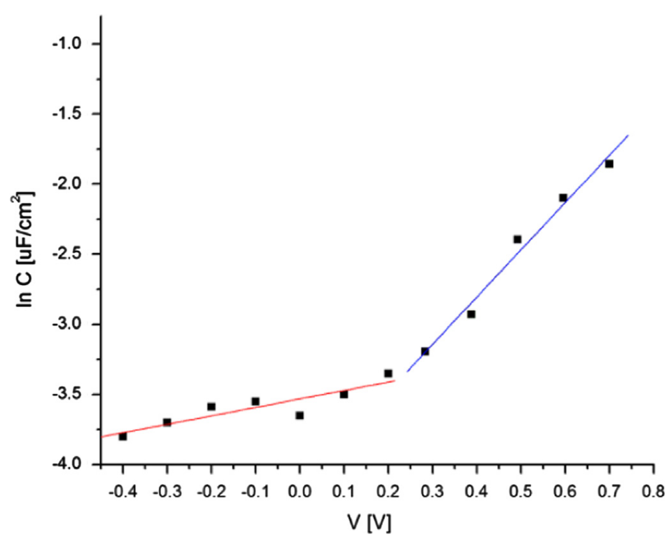

Fig. 9. The semi logarithmic C–V characteristic.

$$\ln C_d = \ln\left(\frac{\tau e}{2kT} I_o\right) + \frac{e}{nkT} V_a \tag{18}$$

The ideality factor of the diode can be determined using the slope of the linear dependence given by the Eq. (18).

The applied voltage for the first region is under 0.2 V. The transition capacitance is dominant for this region.

The junction voltage and the doping density, can be determined using the linear dependence $1/C^2 - V$ called Mott–Schottky plot, obtained from Eq. (1). The doping density can be determined using the slope of the linear dependence and the junction voltage can be determined using the intersections with the y axes.

3.3. Methods to determine the dynamic resistance of solar cells

Method 9 – Thongpron et al. [22] developed a method which allows for the determination of the dynamic resistance, of the series resistance of the solar cell and of the module under both illumination and dark conditions. In this method, the one diode model is used under illumination conditions, Eq. (19) [5].

$$I = I_{ph} - I_o\left(e^{\frac{V+IR_s}{nV_T}} - 1\right) - \frac{V+IR_s}{R_{sh}} \tag{19}$$

Eq. (19) can be customized for the open circuit voltage in Eq. (20), for the short circuit current in Eq. (21) and for a value of the current, I_1, in Eq. (22).

$$I_{ph} = I_o\left(e^{\frac{V_{oc}}{nV_T}} - 1\right) + \frac{V_{oc}}{R_{sh}} \tag{20}$$

$$I_{sc} = I_{ph} - I_o\left(e^{\frac{I_{sc}R_s}{nV_T}} - 1\right) - \frac{I_{sc}R_s}{R_{sh}} \tag{21}$$

$$I_1 = I_{ph} - I_o\left(e^{\frac{V_1+I_1R_s}{nV_T}} - 1\right) - \frac{V_1+I_1R_s}{R_{sh}} \tag{22}$$

The voltage V_1 can be written from Eqs. (20)–(22) as follows:

$$V_1 = nV_T \ln\left[\frac{R_{sh}(I_{ph}+I_o-I_1)}{R_{sh}I_o} - I_1R_s\right] - I_1R_s \tag{23}$$

The series resistance can be determined using Eq. (23) for two points of the I–V characteristic of the solar cell:

$$R_s = \frac{V_1-V_2}{I_2-I_1} - \frac{nV_T}{I_2-I_1}\ln\left[\frac{R_{sh}(I_{ph}+I_o-I_1)-R_sI_1}{R_{sh}(I_{ph}+I_o-I_2)-R_sI_2}\right] \tag{24}$$

Eq. (24) can be rewritten using the following approximations $R_{sh} \gg R_s$, $I_{ph} \approx I_{sc}$ and the ideality factor of diode equal to 1.

$$R_s = \frac{V_1-V_2}{I_2-I_1} - \frac{V_T}{I_2-I_1}\ln\frac{(I_{sc}+I_o-I_1)}{(I_{sc}+I_o-I_2)} \tag{25}$$

The dynamic resistance of the solar cell can be calculated using Eq. (26):

$$R_d = \frac{V_T}{I_2-I_1}\ln\frac{(I_{sc}+I_o-I_1)}{(I_{sc}+I_o-I_2)} \tag{26}$$

Using the short circuit and open circuit conditions the photogenerated current and the reverse saturation current can be determined [22].

In dark conditions the photogenerated current is zero, the series resistance can be calculated using Eq. (27) and the dynamic resistance using Eq. (28), obtained in the same manner as under illumination conditions:

$$R_s = \frac{V_T}{I_2-I_1}\ln\frac{(I_o+I_1)}{(I_o+I_2)} - \frac{V_1-V_2}{I_2-I_1} \tag{27}$$

$$R_d = \frac{V_T}{I_2-I_1}\ln\frac{(I_o+I_1)}{(I_o+I_2)} \tag{28}$$

Method 10 – Wang et al. [23] developed a method to determine the dynamic resistance for the photovoltaic panel under illumination conditions. The method was applied for the multicrystalline silicon photovoltaic panels with different number of cells, for different levels of illumination and temperatures. The dynamic resistance of the photovoltaic panel is determined using the I–V characteristic, the one diode model and equations Eqs. (8) and (29):

$$\frac{dI}{dV} = -\frac{1}{R_{sh}} - \frac{dI}{dV}\frac{R_s}{R_{sh}} - I_o\frac{q}{nkT}\left(1+\frac{dI}{dV}R_s\right)e^{\frac{q(V+IR_s)}{nkT}} \tag{29}$$

where I_o is calculated with Eq. (30), R_s is calculated with Eq. (31), R_{sh} is calculated with Eq. (32) and the value of n is 1 when the diffusion current dominates and 2 when the recombination current dominates:

$$I_o = \left(I_{sc} - \frac{V_{oc}}{R_{sh}}\right)e^{\frac{-qV_{oc}}{nkT}} \tag{30}$$

$$R_s = R_{so} - \frac{1}{I_o}e^{\frac{-qV_{oc}}{nkT}}, \quad R_{so} = -\left(\left.\frac{dI}{dV}\right|_{V=V_{oc}}\right)^{-1} \tag{31}$$

$$R_{sh} = -\left(\left.\frac{dI}{dV}\right|_{I=I_{sc}}\right)^{-1} \tag{32}$$

The nonlinear differential equation to determine the dynamic resistance can be solved using the finite element method [23].

4. Discussion

4.1. Methods analysis

This article outlines ten methods to determine the dynamic parameters of solar cells, such as R_d, C_d, C_t. The static parameters, like R_s, R_{sh}, n, I_o as well as the time constant, the junction voltage, the lifetime and the doping density can also be calculated.

The analysis of the solar cells dynamic parameters can be made in the frequency domain, as described in methods 1, 2, 5 and in the time domain analysis as described in methods 3, 4. These methods allow for the determination of the ac parameters of the solar cells. Table 1 presents a comparison of the ac parameters obtained by impedance spectroscopy using the sinusoidal wave signal (*IS*) and the time domain technique (*T*) for a silicon solar cell.

The ac signal which is superposed on the reverse bias or forward bias can be sinusoidal, triangular or square wave signal. Shorter time periods for the measurements are assured by using the square wave signal superposed, as the measurement steps are reduced. Table 2 presents a comparison of the ac parameters obtained by impedance spectroscopy using the sinusoidal wave signal (Sin) and the square wave signal (Squ) for a silicon solar cell.

The first four methods may be applied in order to determine all the ac parameters of solar cells. These methods also allow for the determination of the dc parameters such as the series and shunt

Table 1
AC parameters of the solar cell obtained by the impedance spectroscopy and the time domain technique.

Solar cell	Condition	Forward bias voltages (V)	R_s [Ω]		R_p [Ω]		C_p [μF]		Comments	Ref.
			IS	T	IS	T	IS	T		
Monocrystalline Si, 4 cm^2	Dark, 25 °C	0.2	–	0.54	28.4	36.59	0.24	0.22	There is a good agreement between the parallel capacitance measured with impedance spectroscopy and time domain technique up to 0.3 V. The matching above 0.3 V is worse, because the capacitance depends on the measurement method and for 0.3–0.5 V the transition and the diffusion capacitance coexist. The matching for R_p is good	[14]
		0.3			10.35	8.05	0.27	0.29		
		0.4			3.39	1.95	0.28	0.46		
		0.45			1.82	1.1	0.39	0.83		
		0.5			0.62	0.67	0.66	1.36		

Table 2
AC parameters of the solar cell obtained by the impedance spectroscopy using the sinusoidal wave signal and the square wave signal.

Solar cell	Condition	Forward bias voltages (V)	R_s [Ω]		R_p [Ω]		C_p [μF]		Comments	Ref.
			Sin	Squ	Sin	Squ	Sin	Squ		
Monocrystalline Si, 10 cm/10 cm	Dark, 25 °C	0.2	0.356	0.352	15.53	15.53	3.33	3.19	R_s remain the same for all bias voltages	[4]
		0.3			4.71	4.9	4.01	3.95	It can be observed the values obtained for the ac parameters by the sinusoidal and square wave used in impedance spectroscopy are very closed	
		0.4			1.39	1.4	4.87	4.82		

resistance and the reverse saturation current. The fifth, the sixth and the seventh methods allow for the determination of only the capacitance of the solar cell. The dynamic and the series resistance of the solar cell can be determined using the ninth and the tenth methods. Moreover the tenth method allows for the determination of the R_{sh} and I_o. The eighth method describes the dependence between the solar cell capacitance and the reverse and forward applied voltage. The ideality factor of diode, junction voltage, lifetime and the doping density can be calculated using the linear dependences, Eqs. (16) and (1).

Although the impedance spectroscopy is a very powerful and quite accurate technique to determine the ac parameters of the solar cell, it uses expensive devices. The experimental set-up consists of ECI – electrochemical interface using as potentiostat, with FRA – frequency response analyzer (ex. Solarton, Autolab, Zahner, etc.), PC – personal computer and DUT – solar cell. The experimental set-up in case of the time domain technique and for the fifth method is less expensive than for the impedance spectroscopy technique. The low frequency oscillographic method has other advantages: it is easily made and the dc bias is not necessary.

Statistically, the impedance spectroscopy is the most widely used method to determine the ac parameters of the solar cells, even if it uses expensive apparatus, because:

- It is generally accepted to analyse the dynamic behavior of all solar cells, especially the organic and inorganic solar cell.
- The devices for the impedance spectroscopy have the software which allows to plot and to analyse the Nyquist diagram.
- The user can chose the proper equivalent circuit for the solar cell from the existing ones or he can build the best circuit in function of the diagram.
- Using the chosen equivalent circuit the diagram can be fitted to determine the ac parameters.

Generally, the photovoltaic modules operate in field conditions and it is very important to measure and analyze the ac parameters of the solar cells and the photovoltaic panels at different levels of illumination and different temperatures [3,10,15,19,24,25], even if most methods use the dark conditions.

There are reports which present the comparison between some dc parameters obtained from the methods in the static regime dc and the dynamic regime ac [36]. The series resistance and the ideality factor of diode obtained from the static and dynamic regime have a good matching for high forward bias. Moreover, in dynamic regime the dependence of the series resistance on voltage can be obtained.

The study of the solar cell behavior in dynamic regime is also made with admittance of spectroscopy. The information obtained using the impedance and admittance is exactly the same because they are reciprocal functions [10,27]. In general, the admittance spectroscopy is used with reverse voltage and offers information about energy levels of the majority of carrier traps and trap densities of states [10].

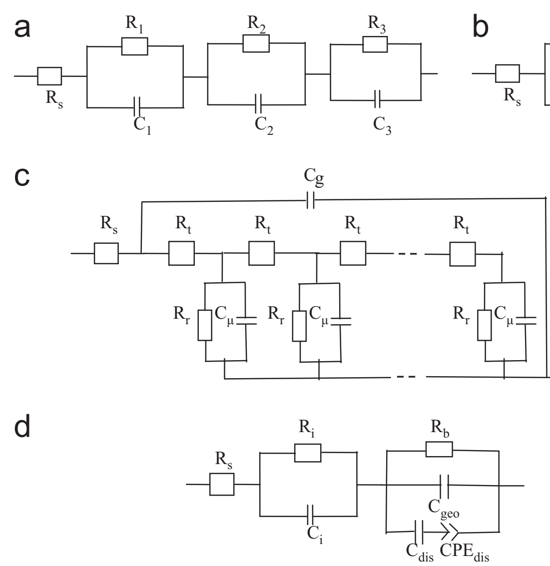

Fig. 10. The ac equivalent circuit for solar cells.

4.2. AC complex equivalent circuits for new solar cells

The capacitance of the solar cell is measured directly by the fifth, the sixth and the seventh methods, while through the impedance spectroscopy technique it is determined indirectly from the fitting procedure of the Nyquist plot (impedance loci) using the equivalent circuit of the solar cell. The accuracy of the fitting procedure depends on the choice of the equivalent circuit and especially on the initial values of the fitting parameters and the confidence interval. The simple equivalent circuit presented in Fig. 3 cannot describe very well the dynamic behavior of all the solar cells. The most important equivalent circuits used for fitting and for determining the parameters of the solar cells, are:

- The RC circuit-is the simplest equivalent circuit of the solar cells, see Fig. 3. It has to be modified in function of the Nyquist diagram, for each semicircle an impedance feature ($R\|C$) is added [28], Fig. 10a. The Nyquist diagram for dye-sensitized solar cell – DSSC is presented in Fig. 11. This implies that there are three impedances, so the equivalent circuit has three components $R\|C$: Z_1 – related to the charge-transfer processes occurring at the Pt counter electrode, Z_2 – corresponding to the diode-like behavior in DSSC and Z_3 – is related to the diffusion of iodide and trioxide within the electrolyte [29,30]. The series resistance is the sum of the R_2 which represents the sheet resistance of the TCO glass substrate of the solar cell, R_1 and R_3.
- the R-CPE circuit-is obtained from the RC circuit by replacing the capacitor with a constant phase element to compensate the non-homogeneities such as surface states, porosities, etc. [31,32], see Fig. 10b. This circuit is proper for organic and polymer solar cells. The circuit can be more complex in function of the semicircles number.

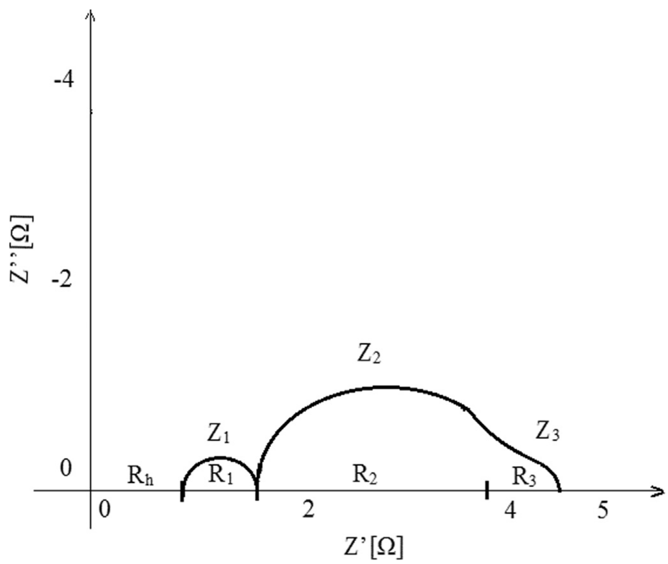

Fig. 11. The impedance loci (Nyquist diagram) for DSSC.

- the TL circuit-is the transmission line circuit for the diffusion-recombination mechanism, Fig. 10c. R_s is the series resistance, R_r is the recombination resistance, R_t is the transport resistance, C_μ represents the chemical capacitance and the C_g represents the dielectric contribution of the diode [33]. This equivalent circuit can be used especially for bulk heterojunction (BHJ) solar cells and DSSC.
- Ecker et al. developed a complex equivalent circuit to describe the behavior of the organic solar cell with TiO_x interlayer [34], Fig. 10d. The RC element is for TiO_x layer and the final part of the circuit describes the transport in the polymer:fullerene active layer.

4.3. Applications of ac parameters

It is well known that the temperature influences the parameters of the solar cells. The *I–V* characteristic of the solar cell has to be measured very quickly to avoid the influence of the temperature. The necessary time to measure the *I–V* characteristic of solar cells is limited by the influence of the capacitance, especially for thin film solar cells and DSSC. Tian et al. show in their study that the lower limit for the necessary time to measure the *I–V* characteristic for dye sensitized solar cell is 200 ms [35].

The determining of the ac parameters of the PV panel is very useful to improve the power converter's performance.

The capacitance of the solar cell influences the performance of the photovoltaic regulators. These have to switch at high frequency where the ripple voltage of the switching regulators increases due to the capacitance of the solar cells [36]. The new solar cells as multi-junction have a high parasitic capacitance which produces new problems as deteriorating the electromagnetic compatibility performance, large current spike produced at MOSFET turning on, etc. [37].

Kim et al. conclude that the performance of the single phase inverter can be increased by limiting until 20% the level of 120 Hz ripple current ratio, [38]. The power loss due to interaction between the 120 Hz ripple current and the 120 Hz AC impedance of the solar cell can be calculated in function of the ac parameters with the following equation [26]:

$$P_{l\_120\ \mathrm{Hz}} = \left(\frac{I_{r\_120\ \mathrm{Hz}}}{\sqrt{2}}\right)^2 \cdot \left(R_{s\_120\ \mathrm{Hz}} + \frac{R_{p\_120\ \mathrm{Hz}}}{\omega^2 R^2{}_{p\_120\ \mathrm{Hz}} C^2{}_{p\_120\ \mathrm{Hz}} + 1}\right) \tag{33}$$

where $I_{r\_120\ \mathrm{Hz}}$ is the 120 Hz ripple current and $R_{s\_120\ \mathrm{Hz}}$, $R_{p\_120\ \mathrm{Hz}}$, $C_{p\_120\ \mathrm{Hz}}$ are the ac parameters at 120 Hz.

The main goal of the photovoltaic panel in grid-connected photovoltaic power systems is to work at maximum power regardless of the illumination levels and panels temperature [39]. Using the ninth or the tenth method, the dynamic resistance at the maximum power point can be determined and using the the impedance matching method the MPP of the panel can be obtained [23].

5. Conclusions

The ten methods which were developed in the last 15 years by various researchers to determine the ac parameters of a solar cell were critically presented, assessed and discussed in this review paper. The methods allow for the determination of the ac parameters such as the diffusion capacitance C_d, the transition capacitance C_t and the dynamic resistance of diode R_d, but also some dc parameters such as the series resistance R_s, the ideality factor of diode n, the reverse diode saturation current I_o and the shunt resistance R_{sh}. The methods presented are classified into four main groups. In the first group there are the methods which allow determining all the ac parameters using the frequency domain technique and the second group includes methods which use the time domain technique to determine the ac parameters of the solar cells. The third group includes the methods which allow determining only one ac parameter as capacitance or dynamic resistance. The fourth group uses the various dependence of the solar cell capacitance to determine the ideality factor of diode n, the minority carrier lifetime, the doping density and the junction voltage.

One may choose the most suitable method to analyze the solar cells in terms of the dynamic regime according to the assessment of the methods outlined in this paper. Attention should be paid in order to avoid the errors in the fitting procedure by using the proper equivalent ac circuit and in the measurement of the *I–V* characteristic for thin film, DSSC and other new type of solar cells.

The understanding of the behavior of the solar cells and photovoltaic panels in dynamic regime is mandatory to design very good solar array regulators and invertors.

Acknowledgments

This work was supported by a Grant of the Romanian National Authority for Scientific Research and Innovation, CNCS – UEFISCDI, Project number PN-II-RU-TE-2014-4-1083.

References

[1] Sawin JL, Sverrisson F. Renewables 2014 global status report, REN21 Secretariat, Paris, France; 2014.
[2] Cotfas DT, Cotfas PA, Kaplanis S. Methods to determine the dc parameters of solar cells: A critical review. Renew Sustain Energy Rev 2013;28:588–96.
[3] Schlosser V, Ghitas A. Measurement of silicon solar cells ac parameters. In: Proceedings of the ARSEC conference Bahrain; 2006.
[4] Chenvidhya D, Kirtikara K, Jivacate C. A new characterization method of the solar cell dynamic impedance. Sol Energy Mater Sol Cells 2003;80:459–64.
[5] Anil Kumar R, Suresh MS, Nagaraju J. Measurement and comparison of AC parameters of silicon (BSR and BSFR) and gallium arsenide (GaAs/Ge) solar cell used in space application. Sol Energy Mater Sol Cells 2000;60:155–66.
[6] Anil Kumar R, Suresh MS, Nagaraju J. Facility to measure solar cell ac parameters using an impedance spectroscopy technique. Rev Sci Instrum 2001;72:3422–6.
[7] Johnson J, Schoenwald D, Kuszmaul S, Strauch J. Creating dynamic equivalent PV circuit models with impedance spectroscopy for arc fault modeling. June. Sandia National Laboratories; 2011.

[8] Kumar S, Sareen V, Batra N, Singh PK. Study of *C–V* characteristics in thin n^+-p-p^+ silicon solar cells and induced junction n-p-p^+ cell structures. Sol Energy Mater Sol Cells 2010;94:1469–72.

[9] Chenvidhya D, Kirtikara K, Jivacate CPV. Module dynamic impedance and its voltage and frequency dependencies. Sol Energy Mater Sol Cells 2005;86:243–51.

[10] Mora-Seró I, Garcia-Belmonte G, Boix PP, Vázquez MA, Bisquert J. Impedance spectroscopy characterisation of highly efficient silicon solar cells under different light illumination intensities. Energy Environ Sci 2009;2:678–86.

[11] Suresh MS. Measurement of solar cell parameters using impedance spectroscopy. Sol Energy Mater Sol Cells 1996;43:21–8.

[12] Chenvidhya D, Limsakul C, Thongpron J, Kirtikara K, Jivacate C. Determination of solar cell dynamic parameters from time domain responses. In: Proceedings of the technical digest of the 14th international photovoltaic science and engineering conference PVSEC14, Bangkok, Thailand 2004.

[13] Anil Kumar R, Suresh MS, Nagaraju J. Time domain technique to measure solar cell capacitance. Rev Sci Instrum 2003;74:3516.

[14] Deshmukh MP, Anil Kumar R, Nagarajua J. Measurement of solar cell ac parameters using the time domain technique. Rev Sci Instrum 2004;75:2732–5.

[15] Deshmukh MP, Nagaraju J. Measurement of silicon and GaAs/Ge solar cells ac parameters. Sol Energy 2005;78:1–4.

[16] Hough TP. Trends in solar energy research. Nova Science Publishers Inc; 2006.

[17] Millman J, Halkias CC. Integrated electronics: analog and digital circuits and systems. New Delhi: Tata McGraw Hill; 1972.

[18] Twarowski AJ, Albrecht AC. Depletion layer studies in organic films: low frequency capacitance measurements in polycrystalline tetracene. J Chem Phys 1979;70(5):2255–61.

[19] Mandal H, Nagaraju J. GaAs/Ge and silicon solar cell capacitance measurement using triangular wave method. Sol Energy Mater Sol. Cells 2007;91:696–700.

[20] Mandal H, Saha S. An improved technique of capacitance measurement of solar cells. In: Proceedings of the third international conference on computer, communication, control and information technology (C3IT), Hooghly, India; 2015.

[21] Jeevandoss CR, Kumaravel M, Jagadeesh Kumar V. A novel measurement method to determine the *C–V* characteristic of a solar photovoltaic cell. IEEE Trans Instrum Meas 2011;60:1761–7.

[22] Thongpron J, Kirtikara K, Jivacatea C. A method for the determination of dynamic resistance of photovoltaic modules under illumination. Sol Energy Mater Sol Cells 2006;90:3078–84.

[23] Wang JC, Shieh JC, Su YL, Kuo KC, Chang YW, Liang YT, et al. A novel method for the determination of dynamic resistance for photovoltaic modules. Energy 2011;36:5968–74.

[24] Garland JE, Crain DJ, Roy D. Impedance spectroscopy coupled with voltammetry for quantitative evaluation of temperature and voltage dependent parameters of a silicon solar cell. Sol Energy 2011;85:2912–23.

[25] Anil Kumar R, Suresh MS, Nagaraju J. GaAs/Ge solar cell AC parameters under illumination. Sol Energy 2004;76:417–21.

[26] Crain DJ, Rock SE, Garland JE, Roy D. Comparison of D.C and A.C electro-analytical methods for measuring diode ideality factors and series resistances of silicon solar cells. Curr Appl Phys 2013;13:2087–97.

[27] Bayhan H, Kavasoglu AS. Admittance and impedance spectroscopy on Cu(In, Ga)Se_2 solar cells. Turk J Phys 2003;27:529–35.

[28] Rock SE, Shi X, Garland JE, Roy D. Experimental considerations for temperature controlled measurements of fast charge recombination times in dye sensitized solar cells using open circuit voltage decay and impedance spectroscopy. Measurement 2014;53:71–82.

[29] Guliani R, Jain A, Kapoor A. Exact analytical analysis of dye-sensitized solar cell: Improved method and comparative study. Open Renew Energy J 2012;5:49–60.

[30] Han L, Koide N, Chiba Y, Islam A, Mitate T. Modeling of an equivalent circuit for dye-sensitized solar cells: improvement of efficiency of dye-sensitized solar cells by reducing internal resistance. Comptes Rendus Chimie 2006;9:645–51.

[31] Perrier G, de Bettignies R, Berson S, Lemaitre N, Guillerez S. Impedance spectrometry of standard and inverted P3HT: PCBM organic solar cells. Sol Energy Mater Sol Cells 2012;101:210–66.

[32] Romero B, del Pozo G, Arredondo B, Reinhardt JP, Sessler M, Wurfel U. Circuital model validation for S-shaped organic solar cells by means of impedance spectroscopy. IEEE J Photovolt 2015;5:234–7.

[33] Garcia-Belmonte G, Munar A, Barea EM, Bisquert J, Ugarte I, Pacios R. Charge carrier mobility and lifetime of organic bulk heterojunctions analysed by impedance spectroscopy. Organ Electron 2008;9:847–51.

[34] Ecker B, Egelhaaf HJ, Steim R, Parisi J, von Hauff E. Understanding S-shaped current – voltage characteristics in organic solar cells containing a TiO_x interlayer with impedance spectroscopy and equivalent circuit analysis. J Phys Chem C 2012;116:16333–7.

[35] Tian H, Zhang J, Wang X, Yu T, Zou Z. Influence of capacitance characteristic on *I–V* measurement of dye-sensitized solar cells. Measurement 2011;44:1551–5.

[36] Kumar RA, Suresh MS, Nagaraju J. Effect of solar array capacitance on the performance of switching shunt voltage regulator. IEEE Trans Power Electron 2006;21:543–8.

[37] Zhu H, Zhang D. Influence of multijunction Ga/As Solar array parasitic capacitance in S3R and solving methods for high-power applications. IEEE Trans Power Electron 2014;29:179–90.

[38] Kim W, Duong V, Nguyen TT, Choi W. Analysis of the effects of inverter ripple current on a photovoltaic power system by using an AC impedance model of the solar cell. Renew Energy 2013;59:150–7.

[39] Jiang JA, Liang YT, Wang JC, Su YL, Kuo KC, Shieh JC. A novel analytical model for determining the maximum power point of thin film photovoltaic module. Prog Photovolt: Res Appl 2014;22:318–31.